so that the charge depends both on the nuclear charge and the number of bonds. Carbon and nitrogen form one more bond than oxygen. Since the ionicity is large, the electron affinity of the ligand is important for the size of the dissociation energy, however, and for the diatomic molecules, NiN is much more weakly bound than NiC and NiO. For the same reason Ni_5N is more weakly bound than the other clusters, but here the larger ionicity and covalency nearly compensate for the poor electron affinity. Carbon forms the strongest bonds both in the diatomic molecule and in the clusters since both the covalency and the electron affinity are large.

Experimentally carbon and nitrogen are found to adsorb close to the surface of Ni(100) whereas oxygen adsorbs further out. The reasons for this different behavior are twofold. First, the covalency to the second-layer nickel atom is much smaller for oxygen, which in turn is due to an almost doubly occupied $2p_z$ orbital (pointing down toward the surface) for oxygen, which cannot form covalent bonds to the second-layer nickel atom. For both carbon and nitrogen the $2p_z$ orbital is far from doubly occupied. This difference between carbon and nitrogen on the one hand and oxygen on the other can be seen in the overlap populations already rather far above the surface. The second reason for the larger force to reconstruct the surface for carbon and nitrogen compared to oxygen is that the ionicity increases much more for the former atoms as the atom penetrates the surface. This again is connected with the occupation of the $2p_z$ orbital for oxygen which already at a large height above the surface becomes almost doubly occupied and therefore cannot accommodate more charge as the atom moves down toward the surface.

The final geometries for Ni_5X are very similar for all three adsorbates, both after a full geometry optimization as well as after an optimization with the cluster geometry fixed. Oxygen consequently also penetrates the surface for these clusters but gains much less energy by doing so than carbon and nitrogen. On a real surface the restoring forces from neighboring atoms are strong enough to keep oxygen outside but cannot resist the stronger force from carbon and nitrogen.

Registry No. NiC, 12167-08-7; NiN, 54485-02-8; NiO, 1313-99-1; Ni_5C, 112138-30-4; Ni_5N, 112138-31-5; Ni_5O, 108599-79-7; C, 7440-44-0; N, 17778-88-0; O, 17778-80-2; Ni, 7440-02-0.

Propensity Rules for Vibration–Rotation-Induced Electron Detachment of Diatomic Anions: Application to $NH^- \rightarrow NH + e^-$

Grzegorz Chalasinski,[†] Rick A. Kendall,[‡] Hugh Taylor, and Jack Simons*

Department of Chemistry, University of Utah, Salt Lake City, Utah 84112 *(Received: August 14, 1987)*

The vibration–rotation-induced electron detachment (VRIED) of diatomic anions has recently become accessible to detailed experimental analysis. Continuing our efforts in this area of nonadiabatic couplings, we attempt to establish more specific angular momentum propensity rules for such processes. In particular, we show how characteristics of the final electronic state may be predicted depending on the symmetry of the initial state and the symmetry of the vibrational or rotational motion that causes the ejection of the electron, and we show how the rates of electron ejection should vary with rotational quantum number. The rotational structure of the VRIED event recently reported by Neumark et al. for NH^- (*J. Chem. Phys.* **1985**, *83*, 4364) is rationalized without our model.

I. Introduction

The vibration–rotation spectroscopy of negative ions has become a rapidly developing field due to the development of new ion sources and the application of modern techniques of tunable laser spectroscopy,[1] fast ion beams, and other ion modulation techniques.[1,2] One of the first anions whose vibrational and rotational structure was studied by these techniques was NH^-.[3] The infrared vibration–rotation spectrum of NH^- was obtained by autodetachment spectroscopy in a coaxial laser–ion beam spectrometer. Rotational transitions within the $v = 0$ to $v = 1$ vibrational absorption of NH^- were sampled, and subsequent autodetachment was observed. The non-instrument-limited line widths of these autodetachment resonance peaks revealed some of the dynamics of the autodetachment process. In particular, the observed increase of the autodetachment rate with rotational energy was much faster than expected if vibrational-to-electronic energy transfer were the primary detachment mechanism (which might be anticipated because most of the energy is in the $V = 1$ vibrational degree of freedom). Moreover, the experimental data suggest that transitions in which the rotational quantum number decreases by a single unit dominate the ejection process. The nature of the p_π orbital of NH^- from which detachment occurs and the fact that this orbital is not strongly affected by vibrational motion suggest that rotational rather than vibrational motion could provide a more efficient avenue for energy transfer to the electronic degrees of freedom. Part of the purpose of this paper is to examine the relative roles of vibrational and rotational motion in this process.

The conceptual framework for vibration–rotation-assisted autoionization in Rydberg states of neutral molecules was formulated by Berry over 20 years ago.[4] For negative ions this treatment has been extended by Simons et al.[5-8] The present paper represents a continuation of these earlier studies, and its purpose is to derive qualitative rotational propensity rules for vibration–rotation-induced electron detachment (VRIED) in the particular

[†] Permanent address: Department of Chemistry, University of Warsaw, Pasteura 1, 02-093 Warsaw, Poland.

[‡] University of Utah Graduate Research Fellow.

(1) Jones, P. L.; Mead, R. D.; Kohler, B. E.; Rosner, S. D.; Lineberger, W. C. *J. Chem. Phys.* **1980**, *73*, 4419. Hefter, U.; Mead, R. D.; Schulz, P. A.; Lineberger, W. C. *Phys. Rev. A* **1983**, *28*, 1479.

(2) Bae, Y. K.; Cosby, P. C.; Peterson, J. R. *Chem. Phys. Lett.* **1986**, *126*, 266. Tack, L. M.; Rosenbaum, N. H.; Owrutsky, J.; Saykally, R. J. *J. Chem. Phys.* **1986**, *85*, 4222. Gruebele, M.; Polak, M.; Saykally, R. J. *J. Chem. Phys.* **1987**, *86*, 1698. **1987**, *86*, 6631. Rosenbaum, N. H.; Owrutsky, J. C.; Tack, L. M.; Saykally, R. J. *J. Chem. Phys.* **1986**, *84*, 5308.

(3) Neumark, D. M.; Lykke, K. R.; Andersen, T.; Lineberger, W. C. *J. Chem. Phys.* **1985**, *83*, 4364.

(4) Berry, R. S. *J. Chem. Phys.* **1966**, *45*, 1228.

(5) Simons, J. *J. Am. Chem. Soc.* **1981**, *103*, 3971.

(6) Acharya, P. K.; Kendall, R. A.; Simons, J. *J. Am. Chem. Soc.* **1984**, *106*, 3402.

(7) Acharya, P. K.; Kendall, R. A.; Simons, J. *Contrib.-Symp. At. Surf. Phys.* **1984**, *84*, 1.

(8) Acharya, P. K.; Kendall, R. A.; Simons, J. *J. Chem. Phys.* **1985**, *83*, 3888.

0022-3654/88/2092-3086$01.50/0

case of diatomic negative ions. For a diatomic negative ion, a compact expression for the electronic force operator can be obtained in a manner that clearly displays its symmetry and physical content. As shown here, this expression may be employed, in particular, to predict isotope effects or to infer the electronic symmetry of the diatomic molecule-plus-free-electron final state if the symmetries of the anion initial state and neutral-molecule final state are known.

The important feature of the detachment process on which we focus our attention here is its dependence on the anion's and neutral molecule's rotational quantum numbers. Previously, only the special case in which the ejection is *assumed* to carry away no angular momentum was treated,[8] whereas, as pointed out above, the recent experiments on NH^- revealed strong evidence for transitions in which the molecule's rotational state changes. This fact stimulated us to derive analytic expressions for the rotational parts of the general propensity matrix element given in ref 5. In the present treatment of NH^-, we restrict our attention to the Hund case b in which the component of the anion's electronic orbital angular momentum along the diatomic bond axis is strongly coupled to the rotational motion and the spin–orbit interaction is a relatively weak effect. This allows us to *first* couple the electronic orbital angular momentum Λ to the rotation and to then bring in the spin–orbit effects. In fact, we further limit our consideration to species for which the resultant spin–orbit coupling is negligible; that is, we couple Λ to rotation to achieve total angular momentum eigenfunctions, and we ignore subsequent spin–orbit interactions. This is done *not* because we believe spin–orbit effects to be small in most cases of interest but because we wish to focus only on the rotation–electronic orbital angular momentum coupling in this work. An analysis of the resultant rate expressions leads to a framework in terms of which we can interpret the observed rotational structure of the VRIED event.

II. Theoretical Development

Although the derivations carried out in this paper are focused, from the start, on the $NH^- \rightarrow NH + e^-$ system, many qualitative features can be carried over to other diatomic anions. Attempts are made throughout this paper to emphasize such general features.

Initial- and Final-State Wave Functions. Let us begin by describing the coupled electronic–vibration/rotation wave functions of the following three species: the NH^- anion, the (hypothetical) [NH,e$^-$] "complex", and the NH-plus-free-electron system. Ignoring the spin–orbit coupling and treating these systems as one active electron coupled to an underlying $^3\Sigma^-$ NH "core", the NH^- anion wave functions can be specified in Hund's case b as

$$|J,M,m\rangle_v = \left(\frac{2J+1}{4\pi}\right)^{1/2} D^{J*}_{M,m}(\alpha,\beta,0)\sum_{nl} C^-_{nl}\psi^-_{nl}(r)\ \psi^-_{lm}(\theta,\phi)\ F^-_{vJ}(R) \quad (1a)$$

where ψ^-_{nl} is the radial part of the NH^- anion's active orbital, $\psi^-_{lm}(\theta,\phi)$ is its angular part expressed in terms of molecule-fixed coordinates r,θ,ϕ; l labels the angular momentum of each of the basis orbitals $\psi^-_{nl}\psi^-_{lm}$ that contribute to the molecular orbital whose angular momentum projection along the bond axis of the molecule is $m\hbar$. C^-_{nl} represents the LCAO–MO coefficients of this active molecular orbital, and the $F^-_{vJ}(R)$ values are vibrational wave functions for the NH^- anion. The angles α and β are the azimuthal and polar angles of the bond axis in the x,y,z lab-fixed coordinate system. Here $D^{J*}_{M,m}(\alpha,\beta,0)[(2J+1)/(4\pi)]^{1/2}$ is the normalized rotational wave function[9,10] for the NH^- system having total (orbital $|m|$ plus rotational M) angular momentum J with projection M along the lab-fixed z axis.

For the [NH,e$^-$] complex in which the "extra" electron is treated as strongly coupled to the bond axis (as in Hund's case b), analogous wave functions are appropriate:

$$|J',M',m'\rangle_{v'} = \left(\frac{2J'+1}{4\pi}\right)^{1/2} D^{J'*}_{M',m'}(\alpha,\beta,0)\sum_{n'l'} C_{n'l'}\psi_{n'l'}\psi_{l'm'}F_{v'J'} \quad (1b)$$

The [NH,e$^-$] "complex" functions do not properly describe the true final states of the decay process. They are introduced merely as a convenient intermediate to facilitate the derivations. The *true* final state of NH-plus-*free*-electron should be described by vector coupling the angular momentum of the free electron to that of the underlying NH species. The $^3\Sigma^-$ NH molecule has no orbital angular momentum, hence its rotational eigenfunctions are given as $[(2\bar{N}+1)/(4\pi)]^{1/2}D^{\bar{N}*}_{\bar{M}_N,0}$. The resultant total angular momentum eigenfunction is then

$$|\bar{J},\bar{M};\bar{N},\bar{l}\rangle_{\bar{v}} = \sum_{\bar{M}_N,\bar{m}} \langle \bar{N}\bar{l}\bar{M}_N\bar{m}|\bar{J}\bar{M}\rangle\left(\frac{2\bar{N}+1}{4\pi}\right)^{1/2} D^{\bar{N}*}_{\bar{M}_N0}(\alpha,\beta,0)\sum_{\bar{n}} C^e_{\bar{n}\bar{l}}\psi^e_{\bar{n}\bar{l}}(r) \times \psi^e_{\bar{l}\bar{m}}(\theta_L,\phi_L)\ F_{\bar{v},\bar{J}} \quad (1c)$$

where θ_L and ϕ_L describe the angular portion of the "extra" electron in the *lab-fixed* x,y,z coordinate system (since the "extra" electron is no longer strongly coupled to the diatomic axis) and $\langle \bar{N}\bar{l}\bar{M}_N\bar{m}|\bar{J}\bar{M}\rangle$ is a vector coupling coefficient.[9,10]

An expansion of these proper final-state wave functions $|\bar{J},\bar{M};\bar{N},\bar{l}\rangle_{\bar{v}}$ in terms of the [NH,e$^-$] functions $|J',M',m'\rangle_{v'}$ allows us to compute rates of decay of specific $|J,M,m\rangle_v$ states of NH^- by first computing $|J,M,m\rangle_v \rightarrow |J',M',m'\rangle_{v'}$ matrix elements and then transforming, using the above-mentioned expansion, to the desired $|J,M,m\rangle_v \rightarrow |\bar{J},\bar{M};\bar{N},\bar{l}\rangle_{\bar{v}}$ rates.

Angular Momentum Considerations and the Nonadiabatic Matrix Elements. The rates of nonadiabatic transitions between states $|J,M,m\rangle_v$ and $|J',M',m'\rangle_{v'}$ induced by vibration/rotation-to-electronic coupling were shown in ref 5 to be related to integrals of the form ${}_{v'}\langle J',M',m'|\vec{\nabla}\cdot\vec{\nabla}|J,M,m\rangle_v$, where the first and second operators

$$\vec{\nabla} = \hat{R}\frac{\partial}{\partial R} + \hat{\beta}\frac{1}{R}\frac{\partial}{\partial\beta} + \hat{\alpha}\frac{1}{R\sin\beta}\frac{\partial}{\partial\alpha}$$

act on the electronic and rotation–vibration components of $|J,M,m\rangle_v$, respectively. It is possible to express $\vec{\nabla}$ in terms of angular momentum operators whose commutation and other properties can then be used to facilitate evaluation of the desired matrix elements. In particular $\vec{\nabla}$ can be written in terms of the rotational angular momentum $\vec{N}$ of the diatomic bond axis:

$$\vec{\nabla} = \hat{R}\frac{\partial}{\partial R} - \frac{i}{\hbar}\frac{\hat{R}\times\vec{N}}{R} \quad (2)$$

The components of $\vec{N}$ in the lab-fixed coordinate system are

$$N_z = -i\hbar\frac{\partial}{\partial\alpha} \quad (3a)$$

$$N_\pm = \pm\hbar\exp(\pm i\alpha)\left(\frac{\partial}{\partial\beta} \pm i\cot\beta\frac{\partial}{\partial\alpha}\right) \quad (3b)$$

Transforming to the molecule-fixed coordinate system with

$$\hat{R} = [\sin\beta\cos\alpha,\ \sin\beta\sin\alpha,\ \cos\beta] \quad (4a)$$

$$\hat{\beta} = [\cos\beta\cos\alpha,\ \cos\beta\sin\alpha,\ -\sin\beta] \quad (4b)$$

$$\hat{\alpha} = [-\sin\alpha,\ \cos\alpha,\ 0] \quad (4c)$$

$\vec{N}$ can be rewritten as

$$N_{\hat{R}} = 0 \quad (5a)$$

$$N_{\hat{\beta}} = \frac{i\hbar}{\sin\beta}\frac{\partial}{\partial\alpha} \quad (5b)$$

$$N_{\hat{\alpha}} = -i\hbar\frac{\partial}{\partial\beta} \quad (5c)$$

The $D^{J*}_{M,m}(\alpha,\beta,\gamma)$ functions are eigenfunctions of the square of the *total* angular momentum $\vec{J} = \vec{N} + \vec{L}$, of the z component J_z, and of the $\hat{R}$ component $J_{\hat{R}}$. In our wave functions $D^{J*}_{M,m}(\alpha,\beta,0)$,

(9) Edmonds, A. R. *Angular Momentum in Quantum Mechanics*; Princeton University Press: Princeton, NJ, 1957.
(10) Brink, D. M.; Satchler, G. R. *Angular Momentum*; Clarendon Press, Oxford University Press: London, 1975.

the angle γ does not occurs since the diatomic has no angular momentum about its bond axis; the only angular momentum about this axis is the electronic orbital angular momentum $\vec{L}$. The well-known expressions for $\vec{J}$ in the lab-fixed coordinate system

$$J_z = -i\hbar \frac{\partial}{\partial \alpha} \tag{6a}$$

$$J_{\pm} = \pm\hbar \exp(\pm i\alpha)\left(\frac{\partial}{\partial \beta} \pm i \cot \beta \frac{\partial}{\partial \alpha} \mp \frac{i}{\sin \beta} \frac{\partial}{\partial \gamma} \right) \tag{6b}$$

can be transformed to the molecule-fixed coordinate system to give

$$J_{\hat{R}} = -i\hbar \frac{\partial}{\partial \gamma} \tag{7a}$$

$$J_{\hat{\beta}} = \frac{i\hbar}{\sin \beta} \frac{\partial}{\partial \alpha} - i\hbar \cot \beta \frac{\partial}{\partial \beta} \tag{7b}$$

$$J_{\hat{\alpha}} = -i\hbar \frac{\partial}{\partial \beta} \tag{7c}$$

Using the properties

$$J_{\hat{R}}\, D^{J*}_{M,m}(\alpha,\beta,\gamma) = m\hbar\, D^{J*}_{M,m}(\alpha,\beta,\gamma) \tag{8a}$$

$$J_{\pm}\, D^{J*}_{M,m}(\alpha,\beta,\gamma) \equiv (J_{\beta} \pm iJ_{\hat{\alpha}})\, D^{J*}_{M,m}(\alpha,\beta,\gamma) = \hbar[J(J+1) - m(m \mp 1)]^{1/2}\, D^{J*}_{M,M\mp1}(\alpha,\beta,\gamma) \tag{8b}$$

one can show that

$$N_{\hat{R}}\, D^{J*}_{M,m}(\alpha,\beta,0) = 0 \tag{9a}$$

$$N_{\pm}\, D^{J*}_{M,m}(\alpha,\beta,0) \equiv (N_{\beta} \pm iN_{\alpha})(\alpha,\beta,0)\, D^{J*}_{M,m}(\alpha,\beta,0) = \hbar[J(J+1) - m(m \mp 1)]^{1/2}\, D^{J*}_{M,m\mp1}(\alpha,\beta,0) - m\hbar \cot \beta\, D^{J*}_{M,m}(\alpha,\beta,0) \tag{9b}$$

Combining all of the above information, one can express the desired nonadiabatic matrix element as follows:

$${}_{v'}\langle J',M',m|\vec{\nabla}\cdot\vec{\nabla}|J,M,m\rangle_{v} = \left(\frac{2J'+1}{4\pi}\right)^{1/2}\left(\frac{2J+1}{4\pi}\right)^{1/2} \times \sum_{\substack{nl \\ n'l'}} C^{*}_{n'l'} \int F^{*}_{v'J'} \int D^{J'}_{M',m}(\alpha,\beta,0) \int \psi^{*}_{n'l'}\psi^{*}_{l'm'}\vec{\nabla}\psi^{-}_{nl}C^{-}_{nl}\psi^{-}_{lm}\, d\vec{r}\cdot \vec{\nabla}\, D^{J*}_{M,m}(\alpha,\beta,0) F_{vJ} R^2 \sin\beta\, dR\, d\beta\, d\alpha = \delta_{JJ'}\delta_{MM'}\{\delta_{m'm}A_{v'Jv} - [B^{+}_{v'Jv}\delta_{m',m+1}[J(J+1) - m(m+1)]^{1/2} + B^{-}_{v'Jv}\delta_{m',m-1}[J(J+1) - m(m-1)]^{1/2}]\} \tag{10}$$

where

$$A_{v'Jv} = \int F^{*}_{v'J}(R) \sum_{nn'l} C^{*}_{n'l} \int \psi^{*}_{n'l} \frac{d}{dR}\psi^{-}_{nl} C^{-}_{nl} r^2\, dr\, \frac{d}{dR} F_{vJ} R^2\, dR \tag{11a}$$

$$B^{\pm}_{v'Jv} = \int F^{*}_{v'J} \sum_{nn'l} C^{*}_{n'l}[l(l+1) - m(m \pm 1)]^{1/2} \times \int \psi^{*}_{n'l}\psi^{-}_{nl} r^2\, dr\, C^{-}_{nl} F_{vJ}\, dR \tag{11b}$$

For the NH^- case, $m = \pm 1$ because of the $^2\Pi$ nature of the electronic state. Moreover, because the π orbital resides primarily on the nitrogen atomic center, the $l = 1$ terms dominate in C^{-}_{nl}. In this case, $B^{+}_{v'Jv}$ vanishes for $m = 1$ and $B^{-}_{v'Jv}$ vanishes for $m = -1$, and the above more general expression reduces to

$${}_{v'}\langle J',M',m|\vec{\nabla}\cdot\vec{\nabla}|J,M,m\rangle_{v} = \delta_{J'J}\delta_{M'M}\{\delta_{m',m}A_{v'Jv} - \delta_{m',0}\delta_{m,-1}B_{v'Jv}[J(J+1)]^{1/2} - \delta_{m',0}\delta_{m,1}B_{v'Jv}[J(J+1)]^{1/2}\} \tag{12}$$

where $B_{v'Jv}$ is given by eq 11b with the $[l(l+1) - m(m \pm 1)]^{1/2}$ factor replaced by $[l(l+1)]^{1/2}$.

Vibration- or Rotation-Assisted Detachment. The final expression (eq 12) for the $|J,M,m\rangle_v$ to $|J',M',m'\rangle_{v'}$ transition matrix elements contains two distinctly different kinds of terms. The $A_{v'Jv}$ elements, which arise for $m' = m$ ($= \pm 1$ for NH^-), originate in the vibrational or radial coupling. Such elements will be large if the rate of change of the anion's active orbital with respect to vibration $(d/dR)\sum_{nl} C^{-}_{nl}\psi^{-}_{nl}$ is large. We note that transitions dominated by these vibrational couplings are expected to display vibrational propensities that vary (approximately) as $\int F^{*}_{v'J'}(R)(d/dR)\, F^{-}_{vJ}(R) R^2\, dR$, where $F_{v'J}$ and F^{-}_{vJ} are the NH and NH^- vibrational wave functions for angular momentum state J. These are *not* conventional Franck–Condon integrals, but integrals that involve the derivative of one of the vibrational wave functions.

The other elements in eq 12 arise from rotational or angular coupling and give rise to $m' = m \pm 1$ ($m' = 0$ for NH^-) transitions in which the electronic angular momentum along the bond axis changes. These $B_{v'Jv}$ elements appear multiplied by $[J(J+1)]^{1/2}$ that give rise to an (approximately) linear variation with the quantum number J. The vibrational propensities that accompany transitions dominated by these couplings should vary (approximately) as $\int F^{*}_{v'J} F^{-}_{vJ}\, dR$, which again are *not* conventional Franck–Condon factors; they have an added factor of R^{-2}.

Transformation from [NH,e⁻] to NH plus Free Electron Rates. Equations 10 and 11 give the matrix elements that couple initial $|J,M,m\rangle_v$ states to "intermediate" $|J',M',m'\rangle_{v'}$ states. As described earlier, these intermediate states, in which the "extra" electron's angular momentum remains coupled to the diatomic bond axis, are not the true final states in the VRIED process. The proper final states $|\bar{J},\bar{M};\bar{N},\bar{l}\rangle_{\bar{v}}$ correspond to a free electron whose angular momentum $\bar{l}$ is vector coupled to the diatomic rotational angular momentum $\bar{N}$. When the definitions of the $|J',M',m'\rangle_{v'}$ and $|\bar{J},\bar{M};\bar{N},\bar{l}\rangle_{\bar{v}}$ states are used, it is relatively straightforward to work out the transformation matrix that connects these two representations:

$${}_{\bar{v}}\langle \bar{J},\bar{M};\bar{l},\bar{m}|J',M',m'\rangle_{v'} = \delta_{JJ'}\delta_{\bar{M}M'}\delta_{\bar{v}v'}\left(\frac{2\bar{N}+1}{4\bar{J}+1}\right)^{1/2}\langle \bar{N},\bar{l},0,m'|\bar{J},m'\rangle C_{\bar{l}} \tag{13a}$$

where

$$C_{\bar{l}} \equiv \sum_{\bar{n}n'} C^{*}_{\bar{n}\bar{l}} \int \psi^{e*}_{\bar{n}\bar{l}}(r)\, \psi_{n'\bar{l}}(r) r^2\, dr\, C_{n'\bar{l}} \tag{13b}$$

is the $\bar{l}$ projection of the [NH,e⁻] "extra" electron's radial wave function onto the "free" electron's radial wave function.

This transformation then allows us to write the desired VRIED matrix elements as

$${}_{\bar{v}}\langle \bar{J},\bar{M};\bar{N},\bar{l}|\vec{\nabla}\cdot\vec{\nabla}|J,M,m\rangle_{v} = \sum_{J',M',m',v'} {}_{\bar{v}}\langle \bar{J},\bar{M};\bar{N},\bar{l}|J',M',m'\rangle_{v'}\, {}_{v'}\langle J',M',m|\vec{\nabla}\cdot\vec{\nabla}|J,M,m\rangle_{v} = \delta_{JJ}\delta_{\bar{M}M}C_{\bar{l}}\left(\frac{2\bar{N}+1}{2J+1}\right)^{1/2}\sum_{m'}\{\delta_{m',m}\langle \bar{N},\bar{l},0,m|\bar{J},m\rangle A_{\bar{v}Jv} - \delta_{m',m+1}\langle \bar{N},\bar{l},0,m+1|\bar{J},m+1\rangle B^{+}_{\bar{v}Jv}[J(J+1) - m(m+1)]^{1/2} - \delta_{m',m-1}\langle \bar{N},\bar{l},0,m-1|\bar{J},m-1\rangle B^{-}_{\bar{v}Jv}[J(J+1) - m(m-1)]^{1/2}\} \tag{14}$$

For the NH^- case, $m = \pm 1$. Recalling that in this case, $B^{+}_{\bar{v}Jv}$ vanishes for $m = 1$ and $B^{-}_{\bar{v}Jv}$ vanishes for $m = -1$, we see that the above expression reduces to

$${}_{\bar{v}}\langle \bar{J},\bar{M};\bar{N},\bar{l}|\vec{\nabla}\cdot\vec{\nabla}|J,M,1\rangle_{v} = \delta_{JJ}\delta_{\bar{M}M}C_{\bar{l}}\left(\frac{2\bar{N}+1}{2J+1}\right)^{1/2}\{\langle \bar{N},\bar{l},0,1|\bar{J},1\rangle A_{\bar{J}Jv} - \langle \bar{N},\bar{l},0,0|\bar{J},0\rangle \times [J(J+1)]^{1/2}B_{\bar{v}Jv}\rangle \tag{15a}$$

$${}_{\bar{v}}\langle \bar{J},\bar{M};\bar{N},\bar{l}|\vec{\nabla}\cdot\vec{\nabla}|J,M,-1\rangle_{v} = \delta_{JJ}\delta_{\bar{M}M}C_{\bar{l}}\left(\frac{2\bar{N}+1}{2J+1}\right)^{1/2}\{\langle \bar{N},\bar{l},0,-1|\bar{J},-1\rangle A_{\bar{v}Jv} - \langle \bar{N},\bar{l},0,0|\bar{J},0\rangle \times [J(J+1)]^{1/2}B_{\bar{v}Jv}\} \tag{15b}$$

Equations 14 and 15 thus provide our final expressions for the $|J,M,m\rangle_v$ to $|\bar{J},\bar{M};\bar{N},\bar{l}\rangle_{\bar{v}}$ matrix elements.

Transitions from NH^- λ-Doublet States. Spectroscopic measurements on NH^- VRIED are able to resolve absorptions from $v'' = 0$ NH^- into various J levels of $v = 1$ NH^-. In fact, the instrumental resolution (<20 MHz) is adequate to resolve transitions into the pairs of λ-doublet states that arise from the pairs of $|J,M,m=\pm1\rangle_v$ states of NH^-. These λ-doublet pairs, whose

energies are split by the rotation–orbital angular momentum coupling, have eigenfunctions, within the Hund case b coupling and with spin–orbit effects being neglected, of the following form for the NH^- $^2\Pi$ state:

$$|J,M,\epsilon\rangle_v = \frac{1}{2^{1/2}}[|J,M,1\rangle_v + \epsilon|J,M,-1\rangle_v] \quad (16)$$

where $\epsilon = \pm 1$ labels the two members of each λ-doublet pair.

In the particular NH^- case at hand, transitions from $|J,M,\epsilon\rangle_v$ initial states to $|\bar{J},\bar{M};\bar{N},\bar{l}\rangle_{\bar{v}}$ final states have nonadiabatic coupling matrix elements that can be obtained from eq 15 and 16:

$$_{\bar{v}}\langle\bar{J},\bar{M};\bar{N},\bar{l}|\vec{\nabla}\cdot\vec{\nabla}|J,M,\epsilon\rangle_v =$$
$$\frac{1}{2^{1/2}}\delta_{\bar{J}J}\delta_{\bar{M}M}C_{\bar{l}}\left(\frac{2\bar{N}+1}{2J+1}\right)^{1/2}\{A_{\bar{v}Jv}\langle\bar{N},\bar{l},0,1|\bar{J},1\rangle \times$$
$$[1+\epsilon(-1)^{\bar{N}+\bar{l}-J}] - [J(J+1)]^{1/2}B_{\bar{v}Jv}\langle\bar{N},\bar{l},0,0|\bar{J},0\rangle(1+\epsilon)\} \quad (17)$$

An interpretation of this result and a comparison with the experimental data on NH^- will be made in section III.

Isotope Effects in VRIED. The nonadiabatic integrals over the *electronic* NH^- and $[NH,e^-]$ wave functions

$$\sum_{\substack{n'n\\ l'l}} C^*_{n'l'}\int \psi^*_{n'l'}\psi^*_{l'm'}\vec{\nabla}\psi^-_{nl}\psi^-_{lm}C^-_{nl}\,d\vec{r} \equiv \vec{M}$$

can be reexpressed[5] in terms of an integral over the *electronic force* operator $\vec{\nabla}h_e$:

$$\vec{M} = \left[E^-(R) - E(R) - \frac{\hbar^2k^2}{2m_e}\right]^{-1} \times \sum_{\substack{n'n\\ l'l}}\int \psi^*_{n'l'}\psi^*_{l'm'}C^*_{n'l'}\vec{\nabla}h_e\psi^-_{nl}\psi^-_{lm}C^-_{nl}\,d\vec{r} \quad (18)$$

where $E^-(R)$ and $E(R)$ are the anion and neutral electronic energies as functions of bond length R and $\hbar^2k^2/2m_e$ is the kinetic energy of the ejected electron. The electronic Hamiltonian h_e for a diatomic species is

$$h_e = \sum_{i=1}^{N}\left[T_e(i) - \frac{Z_ae^2}{r_{ia}} - \frac{Z_be^2}{r_{ib}}\right] \quad (19)$$

where $T_e(i)$ is the kinetic energy operator for the ith electron and r_{ic} is the distance from the ith electron to the cth nucleus whose charge is Z_c. Since $T_e(i)$ is independent of $\vec{R}$ we have

$$\vec{\nabla}h_e = \sum_{i=1}^{N}\vec{\nabla}\left(-\frac{Z_ae^2}{r_{ia}} - \frac{Z_be^2}{r_{ib}}\right) \quad (20)$$

To evaluate eq 20, it is expedient to use spherical polar coordinates of the fixed molecular frame. The nuclear coordinates are then

$$X_a = \frac{M_b}{\mu}R\sin\beta\cos\alpha; \quad X_b = -\frac{M_a}{M_b}X_a$$
$$Y_a = \frac{M_b}{\mu}R\sin\beta\sin\alpha; \quad Y_b = -\frac{M_a}{M_b}Y_a$$
$$Z_a = \frac{M_b}{\mu}R\cos\beta; \quad Z_b = -\frac{M_a}{M_b}Z_a \quad (21)$$

By writing $\vec{\nabla}$ as in eq 2 and carrying out the differentiation in eq 20, after some algebraic manipulations we obtain

$$\vec{\nabla}h_e = \sum_{i=1}^{N}\left[-\frac{Z_ae^2\mu}{M_a}\frac{\vec{r}_{ia}}{r_{ia}^3} + \frac{Z_be^2\mu}{M_b}\frac{\vec{r}_{ib}}{r_{ib}^3}\right] \quad (22)$$

This result is particularly attractive because we express the electronic force operator as a simple function of the position vectors of electrons. Note that although h_e itself is independent of the nuclear masses, $\vec{\nabla}h_e$ is not; hence, we may expect nuclear isotope effects in transitions induced by $\vec{\nabla}h_e$.

The dependence of $\vec{\nabla}h_e$ on the atomic masses M_a and M_b suggests that the rate of the VRIED process will depend on the masses of the isotopes. Consider, for example, NH^- and ND^-. $\vec{\nabla}h_e$ consists of "a-centered" ($\vec{r}_{ia}$) and "b-centered" ($\vec{r}_{ib}$) terms that have different weights, ω_a and ω_b, respectively:

$$\omega_a = \mu/M_a \qquad \omega_a = \mu/M_b$$

If both the initial and final states are described at the single determinant level, the ejected electron is assumed to come from the HOMO of NH^- or ND^-, which is the 1π orbital. This orbital is mainly localized on the N atom, which will be referred to as "a". The "a-centered" term in eq 22 should then dominate (because of the r_{ia}^{-2} factor and because the HOMO is on center a). As shown in ref 5, the rate of VRIED varies as the *square* of the nonadiabatic coupling matrix elements (section II) multiplied by $(2\pi\hbar^3/\mu^2)\rho$, where ρ is the translational density of states for the ejected electron. Hence, the mass dependence of the final rates should arise from $\omega_a^2\mu^{-2}$, or

$$\text{rate} \approx \frac{1}{\mu^2}\left|\frac{\mu}{M_a}\right|^2 = \frac{1}{M_a^2}$$

which is *independent* of the H/D mass ratio. The N^{14}/N^{15} isotopic substitution would give rise to a rate ratio of $|15/14|^2 = 1.15$. In general, we expect large isotope effects when the *active orbital* in the VRIED process is located on the atom being isotopically changed if this atom is light enough so that its isotopes have substantial mass differences.

Further Symmetry Analysis of the Electronic Matrix Elements. The electronic integral given in eq 18 can be symmetry analyzed by substituting eq 22 for $\vec{\nabla}h_e$. The symmetry of $\vec{\nabla}h_e$ is determined by the symmetry of the $\vec{r}_{ia}$ and $\vec{r}_{ib}$ vectors. Within a molecule-fixed coordinate system, it is straightforward to see that the three components of $\vec{r}_{ia}$ and $\vec{r}_{ib}$ belong to σ and π symmetries. The σ component is related to the $\hat{R}$ part of $\vec{\nabla}h_e$, therefore it may be termed "vibrational", whereas the π components are related to $\hat{\beta}$ and $\hat{\alpha}$ and may be termed "rotational".

Given the σ and π symmetries of $\vec{\nabla}h_e$, for a given electronic angular momentum or λ-value of $\sum_{nl}\psi^-_{nl}\psi^-_{lm}C^-_{nl} \equiv \psi^-$ one can determine the possible symmetries of the electronic wave functions $\psi = \sum_{n'l'}C_{n'l'}\psi_{n'l'}\psi_{l'm'}$ for the $[NH,e^-]$ complex and eventually the symmetry of the continuum orbital. To this end let us insert eq 22 into the definition of $\vec{M}$:

$$\vec{M}(R) = \sum_{i=1}^{N}\int\sum_{n'l'}C^*_{n'l'}\psi^*_{n'l'}\psi^*_{l'm'} \times \left(-\frac{Z_ae^2}{r_{ia}^3}\frac{\mu}{M_a}\vec{r}_{ia} + \frac{Z_be^2}{r_{ib}^3}\frac{\mu}{M_b}\vec{r}_{ib}\right)\sum_{nl}C_{nl}\psi_{nl}\psi_{lm}\,d\vec{r}_e\,\Delta E^{-1} \quad (23)$$

This form clearly shows the distance dependence (i.e., r^{-2}) of the $\vec{\nabla}h_e$ operator was well as the mass dependences that arise. In Table I we have worked out examples of this symmetry analyses of $\vec{M}$ for the following three cases:

$$OH^-(^1\Sigma^+) \rightarrow OH(^2\Pi) + e^- \qquad NH^-(^2\Pi) \rightarrow NH(^3\Sigma^-) + e^-$$
$$LiH^-(^2\Sigma) \rightarrow LiH(^1\Sigma^+) + e^-$$

It should be noted that the vibrational ($\hat{R}$) and rotational ($\hat{\beta}$, $\hat{\alpha}$)

TABLE I: Examples of Possible Symmetries of Final States for OH^-, NH^-, and LiH^-

system	initial anion state	$\vec{\nabla}h_e$ component		intermediate "complex" state	final state: neutral molecule[a]	final state: continuum orbital[b]
OH^-	$^1\Sigma^+$	σ	→	$^1\Sigma$	$^2\Pi_\pm$	$l \geq 1$
		$\pi_\pm$	→	$^1\pi_\pm$	$^2\Pi_\pm$	$l \geq 0$
NH^-	$^2\Pi_{\pm 1}$	σ	→	$^2\Pi_\pm$	$^3\Sigma^-$	$l \geq 1$
		$\pi_\pm$	→	$^2\Sigma$	$^3\Sigma^-$	$l \geq 0$
			→	$^2\Delta_\pm$	$^3\Sigma^-$	$l \geq 2$
LiH^-	$^2\Sigma$	σ	→	$^2\Sigma$	$^1\Sigma^+$	$l \geq 0$
		$\Pi_\pm$	→	$^2\pi_\pm$	$^1\Sigma^+$	$l \geq 1$

[a] We assume that the only energetically accessible electronic states of the neutral molecules are $^2\Pi$ for OH, $^3\Sigma^-$ for NH, and $^1\Sigma^+$ for LiH. [b] The smallest value of l that is allowed and which should dominate.

components of $\vec{\nabla}h_e$ connect ψ^- and ψ with $\Delta m = 0,\pm1$. This restriction is important because it enters into the rotational propensity determinations.

It should be noted that the angular momenta predicted for the outgoing electron as in Table I are only the *minimum* values needed to provide consistency in the m' values of the [molecule, e^-] complex and the molecule-plus-free-electron final state. Additional constraints may occur that cause the electron to be ejected *primarily* in higher l waves. For example, in the NH^- case, since the active 1π orbital consists almost entirely of a nitrogen-atom-centered p orbital and since the anion's rotation takes place about a point (the nuclear center of mass) near the nitrogen atom, the rotational coupling produces the [NH,e^-] complex in a $^2\Sigma$ state in which the "extra" electron resides in a p_σ orbital (rather than an s_σ or d_σ orbital). As a result, the transformation from the [NH,e^-] complex to the NH-plus-free-electron state involves an $l = 1$ free electron.

III. Analysis of Propensity Results for NH^-

In the initial infrared absorption process an NH^- anion in $v = 0$ is excited to a particular J rotational level of the $v = 1$ state. In fact, each individual molecular excitation event produces a particular M state of the J rotational level, even if transitions to different λ-doublet members ($\epsilon = \pm1$) are individually resolved. Thus it is proper to speak of each VRIED process as beginning in a single quantum state labeled by its ϵ λ-doublet quantum number as well as its rotational J,M quantum numbers.

In principle, transitions from such a $|J,M,\epsilon\rangle_{v=1}$ initial state to all energetically possible final states contribute to the decay rate. Thus, according to ref 5, the total rate of decay can be expressed as

$$\text{rate} = \frac{2\pi h^3}{\mu^2}\rho \sum_{\bar{v},\bar{J},\bar{N},\bar{l},\bar{M}} |_{\bar{v}}\langle \bar{J},\bar{M};\bar{N},\bar{l}|\vec{\nabla}\cdot\vec{\nabla}|J,M,\epsilon\rangle_v|^2 \qquad (24)$$

Inserting the expression given in eq 17 for the above coupling matrix elements yields

$$\text{rate} = \frac{2\pi h^3}{\mu^2}\rho \sum_{\bar{v},\bar{N},\bar{l}} \frac{1}{2}|C_{\bar{l}}|^2\left(\frac{2\bar{N}+1}{2J+1}\right)|A_{\bar{v}Jv}\langle \bar{N},\bar{l},0,1|J,1\rangle \times [1 + \epsilon(-1)^{\bar{N}+\bar{l}-J}] - [J(J+1)]^{1/2}B_{\bar{v}Jv}\langle \bar{N},\bar{l},0,0|J,O\rangle(1+\epsilon)|^2 \qquad (25)$$

Recall that $A_{\bar{v}Jv}$ arises from radial or vibrational coupling whereas $B_{\bar{v}Jv}$ involves angular or rotational coupling. From eq 11a and 11b it is clear that the J dependences of $A_{\bar{v}Jv}$ and $B^{\pm}_{\bar{v}Jv}$ are weak compared with the J dependence explicitly displayed in eq 25.

The vector coupling coefficients $\langle N,\bar{l},0,0|J,0\rangle$ vanish unless $\bar{N} + \bar{l} - J$ is an even integer. Of course, the three quantum numbers $\bar{N}$, $\bar{l}$, and J must also obey the vector coupling triangle condition. Thus the change in rotational quantum number accompanying the $NH^- \rightarrow NH + e^-$ event must obey $\bar{N} - J = 2p - \bar{l}$. Since $\bar{l} = 1$ was shown to dominate for the NH^- case, we predict that $\bar{N} - J = -1$ ($\bar{N} - J = 1$ is energetically impossible for NH^- because the rotational levels of the $v = 1$ vibrational state of NH^- lie below the corresponding rotational levels of $v = 0$ for NH). Values of $|\bar{N} - J|$ greater than 1 violate the triangle condition if $\bar{l} = 1$ (as in NH^-).

For NH^-, the initial vibrational quantum number v is equal to 1, for which the only accessible final NH vibrational level is $\bar{v} = 0$. Thus the rate expression reduces to

$$\text{rate} \cong \frac{2\pi h^3}{\mu^2}\frac{1}{2}|C_1|^2\left(\frac{2(J-1)+1}{2J+1}\right)|A_{0J1}\langle J\text{-}1,1,0,1|J,1\rangle \times [1 + \epsilon(-1)^0] - [J(J+1)]^{1/2}B_{0J1}\langle J\text{-}1,1,0,0|J,0\rangle(1+\epsilon)|^2 \qquad (26)$$

This rate expression suggests that the $\epsilon = 1$ component of each λ-doublet should decay with a rate that varies with J approximately as $|a - bJ|^2$, where a and b relate to $A_{0J1}\langle J\text{-}1,1,0,1|J,1\rangle$ and $B_{0J1}\langle J\text{-}1,1,0,0|J,0\rangle$, respectively. In the case of NH^-, the 1π molecular orbital is not expected to vary strongly with vibration (i.e., $d\psi^-/dR$ is small), therefore rotational couplings (B_{0J1}) should dominate over vibrational couplings (A_{0J1}). As a result, VRIED rates are expected to vary (approximately) as b^2J^2. The experimental line width data do, in fact, demonstrate a J dependence that can be interpreted as being of the $|a - bJ|^2$ form (for one of the members of each λ-doublet). The photoelectron time-of-flight data also support the prediction of eq 26 that $\bar{N} = J - 1$ transitions should be strongly favored (because $\bar{l} = 1$ dominates).

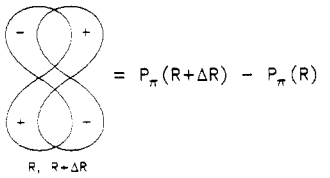

Figure 1. Pictorial representation of the finite difference representation of dP_π/dR.

According to eq 26, the $\epsilon = -1$ component of each λ-doublet pair should have *zero* rate of electron ejection within the approximations that gave this equation. Experimentally it is observed that the rates of VRIED from one member of each λ-doublet are considerably lower and much less J dependent than those of the fast-decaying member. The lack of strong J dependence indicates that the slowly decaying λ-doublet states eject electrons via vibrational coupling rather than by rotational coupling.

To understand how additional contributions to the radial coupling elements can arise, we return to the factor $(d/dR)\bar{\psi}_{nl}\bar{\psi}_{lm}C^-_{nl}$, which enters into eq 11a for $A_{v'Jv}$. The R derivative acts not only on the $C^-_{nl}(R)$ LCAO-MO coefficients (which does not give rise to higher l values) but also on the coordinate origin to which the $\bar{\psi}_{nl}\bar{\psi}_{lm}$ functions are attached. It is straightforward to see (pictorially or analytically) that the R derivative of a p_π orbital centered on the N atom generates a function of d_π symmetry (see Figure 1). The introduction of a d_π component ($l = 2$) then leads to $l = 2$ type π terms in the [NH,e^-] electronic wave function, which in turn leads to dominance of $\bar{l} = 2$ in the final free-electron function. These $\bar{l} = 2$ transitions would indeed give rise (see eq 17) to nonzero VRIED radial coupling rates for $\epsilon = -1$ λ-doublet states because now $(-1)^{\bar{N}+\bar{l}-J} = -1$ for the dominant $\bar{N} - J = -1$ rotational transitions. It should be stressed that exactly the same $\bar{N} - J = -1$ transitions occur both for this (slowly decaying via $\bar{l} = 2$ radial coupling) $\epsilon = -1$ λ-doublet as for the (fast decaying, via $\bar{l} = 1$ angular plus radial coupling) $\epsilon = 1$ λ-doublet. This is consistent with the experimentally observed photoelectron time-of-flight data.

IV. Summary and Conclusions

The rotational angular momentum dependence of the rate of VRIED in diatomic anions has been analyzed within a first-order perturbation theory "golden rule" model. It has been demonstrated that, for diatomics, the electronic force operator $\vec{\nabla}h_e$ consists of two components: a "vibrational" one of σ symmetry and a "rotational" one of π symmetry. Knowing the symmetries of $\vec{\nabla}h_e$, one can easily predict the electronic symmetry of the diatomic molecule-plus-free-electron final state and hence the ejected electron's angular dependence if the symmetry of the neutral-molecule final state is known. The examples of OH^-, NH^-, and LiH^- have been discussed to illustrate the prediction of the symmetry of the outgoing electron wave.

The explicit form of $\vec{\nabla}h_e$ for a diatomic molecule derived in this paper also enables prediction of isotope effects in the VRIED process. In particular, it has been shown that the rate of VRIED should be slightly larger for $^{14}NH^-$ than for $^{15}NH^-$.

Explicit evaluation of the angular terms in the "golden rule" rate expression resulted in establishing angular momentum propensity rules for this process. As applied to VRIED in $^2\Pi$ NH^-, these propensities predict the following: (1) One component of each λ-doublet rotational state in NH^- should decay with a rate whose J dependence varies as $|a - bJ|^2$ and should involve ejection of $\bar{l} = 1$ (p wave) electrons. (2) The other component of each λ-doublet should decay more slowly, should involve ejection of $\bar{l} = 2$ (d wave) electrons, and should vary weakly with J. (3) Both λ-doublet components should be dominated by rotational transitions that involve unit decrease in the rotational quantum

number. All three of these predictions are in agreement with what has been seen experimentally.

The more general conclusions of this analysis include the following: (1) highly non-Franck–Condon vibrational propensities due to the appearance of d/dR and R^{-2} factors in the radial and angular nonadiabatic coupling matrix elements (see 11a and 11b); (2) strong J dependence for one component of each λ-doublet and weak J dependence for the other; (3) propensity for small changes in the rotational quantum number, with the minimum charge determined by the $\bar{l}$ value of the ejected electron; (4) weak J dependence for the vibration-induced rates and strong J dependence for rotation-induced rates.

Acknowledgment. We acknowledge the financial support fo the National Science Foundation (Grants No. CHE-8206845 and CHE-8511307) and the donors of the Petroleum Research Fund, administered by the American Chemical Society. We also acknowledge the Harris Corp. for their generous computer system grant and the National Science Foundation for its San Diego Supercomputer time award. We also thank the San Diego Supercomputer Center for their computer time grant. G.C. thanks the Polish Academy of Sciences within the program CPBP01.12 for their support. R.A.K. thanks the University of Utah for their partial support through the Graduate Research Fellowship program.

An Automatic Grid Generation Scheme for Pseudospectral Self-Consistent Field Calculations on Polyatomic Molecules

Richard A. Friesner

Department of Chemistry, The University of Texas at Austin, Austin, Texas 78712
(Received: August 17, 1987; In Final Form: November 13, 1987)

We describe a stable and efficient approach to generating a reliable polyatomic grid for self-consistent electronic structure calculations using the pseudospectral method. Systematic convergence of spectroscopic constants to the Roothaan Hartree–Fock values as the grid size is increased is demonstrated. The approach offers an estimated 1–2 order of magnitude reduction over alternative numerical self-consistent field algorithms in the number of grid points per atom required to produce accurate results.

I. Introduction

In a series of previous papers,[1-3] a new algorithm for solution of self-consistent electronic structure equations has been proposed and implemented. The algorithm involves a synthesis of conventional quantum chemical techniques with the pseudospectral method,[4] an efficient numerical method originally applied to large-scale hydrodynamic simulations[5] and recently employed in various contexts in chemical physics problems.[6] The essential feature of the approach is use of both a basis set and a numerical grid representation of the solution, allowing accurate evaluation of derivatives and integrals but also permitting multiplications to be carried out efficiently on the physical space grid. The net results for the Hartree–Fock equations are elimination of two-electron integrals and an N^3 scaling of both integral evaluation and Fock matrix assembly, thus potentially yielding 2–3 orders of magnitude reduction in computation time for large molecules.

In ref 3, quantitatively accurate results (as compared to equivalent calculations done via the Roothaan procedure[7]) for the water molecule were obtained for the dissociation energy, force constants, and equilibrium geometry. This demonstrated that the pseudospectral method was capable of achieving the high accuracy reequired for quantum chemical calculations on polyatomic molecules. However, a cumbersome nonlinear optimization procedure was required to achieve these results. Furthermore, this procedure is not easily generalized to large polyatomics. Consequently, a more automated and universal implementation is required if the pseudospectral method is to become a useful quantum chemical approach which is easily applied to a user-specified molecular system.

In this paper, the most difficult step in that direction is taken. The key problem identified in ref 3 is that of automatic grid generation for a polyatomic system. A practical solution to that problem is described below. There are still details of the scheme which can be improved; we expect that such improvement will allow reduction of the number of grid points required. However, the method as depicted should be directly applicable to an arbitrary polyatomic system. The explicit demonstration of this (along with any improvements developed along the way) will appear in subsequent publications. Here, we report results for the water molecule which are analogous in quality to those in ref 3. In contrast to the work reported in that paper, the grid design implemented here is a systematic procedure which should not require reoptimization for each molecular species.

No new timing results are presented here; the principal concern is description of the grid generation algorithm and establishment of accuracy for that algorithm. However, the conclusions regarding the number of grid points per atom, which is a critical parameter in determining the efficiency of any numerical self-consistent field (SCF) method, are in accord with those in ref 3. The requisite number of points is 1 or more orders of magnitude less than that used in previously described numerical schemes, whether for the Hartree–Fock (HF) equations or in the less demanding context of local density theory. The reason such large

(1) Friesner, R. *Chem. Phys. Lett.* **1985**, *116*, 39.
(2) Friesner, R. *J. Chem. Phys.* **1986**, *85*, 1462.
(3) Friesner, R. *J. Chem. Phys.* **1987**, *86*, 3522.
(4) Orszag, S. A. *Stud. Appl. Math.* **1972**, *51*, 253. Orszag, S. A. *Stud. Appl. Math.* **1971**, *50*, 293. Orszag, S. A. *Phys. Rev. Lett.* **1971**, *26*, 1100. Gottlieb, D.; Orszag, S. *Numerical Analysis of Spectral Methods; Theory and Application*; SIAM: Philadelphia, 1977.
(5) Brachet, M. E.; Meiron, D. E.; Orszag, S. A.; Nickel, B. G.; Morf, R. H.; Frisch, V. *J. Fluid Mech.* **1983**, *130*, 411. Patera, A. T. *J. Comput. Phys.* **1984**, *54*, 468. Marcus, P. S. *J. Fluid Mech.* **1984**, *446*, 45. Orszag, S.; Patera, A. T. *Phys. Rev. Lett.* **1980**, *45*, 989. Yakhot, V.; Orszag, S. A.; Pelz, R. B. In *Proceedings of the 9th International Conference on Numerical Methods in Fluid Dynamics*; Springer-Verlag: New York, 1985. Tuckerman, L. S.; Marcus, P. S. *Ibid.* Springer-Verlag: New York, 1985.
(6) Kosloff, D.; Kosloff, R. *J. Comput. Phys.* **1983**, *52*, 35. Gerber, R. B.; Yinnon, A. T.; Kosloff, R. *Chem. Phys. Lett.* **1984**, *105*, 523. Light, J. C.; Hamilton, I. P.; Lill, J. V. *J. Chem. Phys.* **1985**, *82*, 1400. Selloni, A.; Carnevali, P.; Car, R.; Parrinello, M. *Phys. Rev. Lett.*, in press.
(7) Roothaan, C. C. J. *Rev. Mod. Phys.* **1951**, *23*, 69.

0022-3654/88/2092-3091$01.50/0